THE ASTROPHYSICAL JOURNAL, 582:823–829, 2003 January 10

OBSERVATIONS OF C_3 IN TRANSLUCENT SIGHT LINES

TAKESHI OKA,[1] JULIE A. THORBURN,[1] BENJAMIN J. MCCALL,[1,2] SCOTT D. FRIEDMAN,[3] LEWIS M. HOBBS,[1] PAULE SONNENTRUCKER,[3] DANIEL E. WELTY,[1] AND DONALD G. YORK[1]
Received 2002 July 31; accepted 2002 September 16

ABSTRACT

The $A\ ^1\Pi_u \leftarrow X\ ^1\Sigma_g^+$ transition of the simplest polyatomic carbon chain molecule, C_3, at 4051.6 Å has been searched for toward reddened stars where abundant C_2 had been reported and toward other stars with high color excess. Absorption from C_3 has been detected toward 15 stars with color excess $E(B-V)$ from 0.33 to 1.12. The observed C_3 column densities, ranging from 10^{12} to 10^{13} cm^{-2}, are well correlated with the corresponding C_2 column densities, with $N(C_2)/N(C_3) \sim 40$, indicating their close chemical relation. The carbon-rich sight line toward HD 204827 (for which no previous C_2 observation had been reported) has by far the highest C_3 and C_2 column densities. The chemistry of formation of C_3 from C_2 is discussed. A search for the next strongest 020–000 vibronic band was unsuccessful as a result of the low Franck-Condon factor and interference with a stellar line. Searches for C_4 and C_5 were negative.

Subject headings: astrochemistry — ISM: lines and bands — ISM: molecules

1. INTRODUCTION

The recent detection by Maier et al. (2001) of the absorption at 4051.6 Å of C_3 in diffuse interstellar clouds, toward the reddened stars ζ Ophiuchi, 20 Aquilae, and ζ Persei, has demonstrated the abundance of this simplest polyatomic carbon chain molecule, which had been sought in the diffuse interstellar medium for many years (Clegg & Lambert 1982; Snow, Seab, & Joseph 1988; Haffner & Meyer 1995). The obtained C_3 column densities of $(1\text{–}2) \times 10^{12}$ cm^{-2} are higher than the predicted values in the comprehensive model calculations by van Dishoeck & Black (1986) by several orders of magnitude and are closer to that predicted by the simpler calculation of Clegg & Lambert (1982). Subsequently, C_3 has been observed toward the more reddened star HD 210121 with a C_3 column density of 3.8×10^{12} cm^{-2} by Roueff et al. (2002). For many years, optical observations in the diffuse interstellar medium had been limited to atoms and diatomics. However, the recent observations of C_3, along with the infrared observations of H_3^+ (McCall et al. 1998, 2002; Geballe et al. 1999), mark the arrival of polyatomic molecular spectroscopy. Searches for longer carbon chain molecules C_4 and C_5 at 3788.6 and 5109.4 Å, respectively, by Maier, Walker, & Bohlender (2002) in ζ Ophiuchi were negative.

The λ4051.6 band of C_3 was first noted in emission in William Huggins' plate of comet Tebbutt (Huggins 1881, 1882) and has since been observed in many comets (for early works see Bobrovnikoff 1931, 1942). The spectrum was also observed in absorption in photospheres of the N-type carbon star YCVn (McKellar 1948) and other cool stars (for a review see Jørgensen 1994). The carrier of the spectrum was identified to be C_3 in a laboratory experiment by Douglas (1951), and the transition was assigned to $^1\Pi_u \leftarrow {}^1\Sigma_g^+$ by Gausset et al. (1963). The absorption has been seen strongly in CRL 2688 (Crampton, Cowley, & Humphreys 1975), as well as in other carbon-rich protoplanetary nebulae (Hrivnak & Kwok 1999). C_3 has also been observed through its infrared spectrum at 4.9 μm, corresponding to the antisymmetric C—C stretching vibration, in the circumstellar material around the late-type carbon star IRC +10216 (Hinkle, Keady, & Bernath 1988), and through its far-infrared absorption spectrum at 157 μm, corresponding to the anomalously low bending vibration, toward Sagittarius B2 and IRC +10216 (Cernicharo, Goicoechea, & Caux 2000) with the high column densities of 6×10^{15} and 2×10^{16} cm^{-2}, respectively. Recently Giesen et al. (2001) published one line [$R(2)$] of the far-infrared spectrum observed in high spectral resolution with the Kuiper Airborne Observatory that had initially been reported in 1995.

We report here our observations of the C_3 absorption spectrum in the diffuse interstellar medium in translucent sight lines (often defined to have visual extinctions between 1 and 5 mag). The resolving power ($R = 37,500$) of our Astrophysical Research Consortium Echelle Spectrometer (ARCES) is not sufficient to resolve individual rotational lines as was successfully accomplished with the Gecko echelle spectrograph used by Maier et al. (2001; with $R = 121,000$) and by the UV–Visual Echelle Spectrograph used by Roueff et al. (2002; $R = 69,000$), but it allows us to obtain spectra of stars that are fainter in the violet. We have detected the C_3 spectrum toward stars with high color excesses, such as HD 169454 [$E(B-V) = 1.12$] and HD 204827 [$E(B-V) = 1.11$], in contrast to the stars with $E(B-V) = 0.31$–0.33 studied by Maier et al. (2001) and $E(B-V) = 0.40$ by Roueff et al. (2002). The observed C_3 column densities are higher. Although our low instrumental resolution makes the sensitivity of detection considerably lower and does not allow us to determine the temperature of individual clouds accurately, the C_3 column densities can be measured with a reasonable accuracy by comparing observed spectra with simulated spectra.

2. OBSERVATIONS

Observations were carried out using the ARCES spectrometer attached to the 3.5 m telescope at the Apache Point

[1] Department of Astronomy and Astrophysics, University of Chicago, Chicago, IL 60637; t-oka@uchicago.edu.
[2] Department of Astronomy, University of California at Berkeley, 601 Campbell Hall, Berkeley, CA 94720.
[3] Department of Physics and Astronomy, Johns Hopkins University, Baltimore, MD 21218.

TABLE 1
DATA FOR PROGRAM STARS

Star	Name	Type	V	$E(B-V)$	D (pc)[a]	Date (UT)[b]
HD 21483	...	B3 III	7.06	0.56	440	10(18,19)00, 091101, 100801
HD 24398	ζ Per	B1 Ib	2.85	0.31	301	100801
HD 24534	X Per	O9.5 pe	6.10	0.59	590	100801, 110201
HD 26571	...	B9 IIIp	6.12	0.25	140	122601
HD 27778	62 Tau	B3 V	6.36	0.37	223	012000, 120500, 020601
HD 29647	...	B8 IIIp	8.31	1.00	177	020799, 09(08,09,11)01
HD 34078	AE Aur	O9.5 Ve	5.96	0.52	620	120500, 021001
HD 42087	3 Gem	B2.5 Ibe	5.75	0.36	1200	122200
HD 46202	...	O9 V	8.19	0.49	2000	01(20,23)00, 020601, 030501 012702
HD 46711	...	B3 II	9.10	1.04	1200	02(02,04,08,20,21,23)99
HD 53367	...	B0 IVe	6.96	0.74	780	010200, 020601, 012602
HD 147888	ρ Oph D	B5 V	6.74	0.47	136	061000, 05(02,03,06)01
HD 147889	...	B2 V	7.90	1.07	136	02(21,23)99, 040999, 061000, 05(02,03)01, 060201
HD 149757	ζ Oph	O9.5 V	2.56	0.32	140	061000, 050701
HD 169454	...	B1.5 Ia	6.61	1.12	930	101800, 05(30,31)01, 060101, 07(12,13)01
HD 170740	...	B2 V	5.72	0.48	213	060201
HD 172028	...	B2 V	7.83	0.79	380	07(12,13)01, 090501
HD 179406	20 Aql	B3 V	5.34	0.33	160	05(07,30)01, 060101, 070501, 090501
HD 203938	...	B0.5 IV	7.08	0.74	700	081200, 060201
HD 204827	...	B0 V	7.94	1.11	600	09(05,08,09)01, 102901
HD 206267	...	O6 f	5.62	0.53	1000	061700, 081200, 07(12,13)01, 09(09,11)01
HD 207198	...	O9 IIe	5.95	0.62	1000	081300, 09(09,11)01
HD 210121	...	B3 V	7.67	0.40	210	090200, 101900, 120500, 100901
HD 210839	λ Cep	O6 If	5.04	0.57	505	06(17,18)00, 081300

[a] The distances to stars have been estimated by one of us (L. M. H.). For nine of the 24 stars listed for which *Hipparcos* parallaxes of 4 σ precision or better are available, the distances were derived from these parallaxes. For the other 15 stars, the distances were estimated from the photometry, the spectral types, and an adopted value $A_v/E(B-V) = 3.1$ in the usual way.
[b] The date of observation is given in the order of month-day-year.

Observatory (APO). Data reduction was done by using standard IRAF routines as described in detail by Thorburn (2000[4]) and Wang et al. (2002). Because of the observed (Maier et al. 2001) and expected good correlation between column densities of C_2 and C_3, the program stars were chosen from a star sample toward which high column densities of C_2 had been reported. Since its discovery toward Cygnus OB2 No. 12 (Souza & Lutz 1977), ζ Oph (Chaffee & Lutz 1978), and ζ Per (Hobbs 1979), interstellar C_2 has been observed toward over 50 stars. The C_2 column densities, originally reported in many papers, are tabulated in four papers, that is, van Dishoeck & Black (1989), Crawford (1990), Federman et al. (1994), and Gredel (1999).

We have also examined other reddened sight lines with $E(B-V) > 0.4$ for which observations of C_2 had not previously been reported but which might be expected to have high C_2 column densities. In connection with our extensive, ongoing survey of the diffuse interstellar bands, we have obtained spectra of almost all the stars accessible from APO toward which C_2 has been detected and also of many other stars with color excesses between 0.4 and 1.12 mag. Our survey has aimed at achieving a signal-to-noise ratio (S/N) of 1000 near 5800 Å, but we further integrated on selected stars to have high S/N in the violet. Two sight lines for which C_2 had not previously been reported have shown the C_3 absorption lines. Strong C_2 absorption has been observed toward both sight lines. In fact, HD 204827 (which showed by far the highest C_3 column density) belonged to this group of stars. A particularly long integration (9.5 hr) has been used for this sight line.

[4] Available at http://www.apo.nmsu.edu/instruments/echelle.

The observed stars, their spectral types, visual magnitudes, color excesses, distances, and dates of observation are summarized in Table 1. This table is limited to stars toward which C_3 has been detected and those toward which C_2 has been detected for the first time. A total of 39 other sight lines have also been examined as discussed later in § 4.1.

3. SPECTRAL SIMULATION

Since individual rotational lines are not resolved in our observations, we determined C_3 column densities by comparing simulated and observed spectra. For this purpose we used the wavelengths reported by Gausset et al. (1965) and the Hönl-London intensity factors for a perpendicular band ($\Lambda = 1 \leftarrow 0$), i.e., $(J+2)/2(2J+1)$, $\frac{1}{2}$, and $(J-1)/2(2J+1)$ for the R-, Q-, and P-branch lines, respectively.

The distribution of molecular population in individual rotational levels is a complicated problem for nonpolar molecules like C_2 and C_3 since a subtle balance of the radiative and collisional pumping rates and the formation and destruction rates of the molecules needs to be considered (van Dishoeck & Black 1982). Maier et al. (2001) have reported a two-temperature distribution for C_3 in ζ Oph corresponding to a low temperature $T_l = 60$ K for lower rotational levels ($J = 0$–12) and a high temperature $T_h = 230$ K for higher levels with $J \geq 12$. Such a distribution has also been reported for C_2 toward other stars (Lutz & Crutcher 1983). Roueff et al. (2002) applied a much more sophisticated analysis to their observations of C_3 toward HD 210121. In view of the difficulty and uncertainty of such analysis, the lack of rotational resolution in our spectra, and the relatively lower temperature of our sources (see below), we here use the simplest assumption of a one-temperature rotational distribution.

Examples of simulated spectra are compared with the observed spectrum toward HD 204827 in Figure 1. Figure 1*a* shows a simulated spectrum using the resolution of 110,000 used by Maier et al. (2001) at $T = 40$ K. Figure 1*b* gives the same spectrum simulated for our observational conditions, i.e., resolution of 34,000 and S/N of 900. Figure 1*c* shows the observed spectrum of HD 204827. Figure 1*d* shows a simulated spectrum at the same conditions for Figure 1*b*, except that the two-temperature distribution of Maier et al. (2001) is used. The temperature of $T = 40$ K is used in Figures 1*a* and 1*b* because of the observed sharpness of the central *Q*-branch pileup. Simulations at $T_l = 60$ K of Maier et al. (2001) and $T_l = 65$ K of Roueff et al. (2002) yield a considerably broader *Q*-branch feature. In addition, our C_2 spectrum toward this star shows rotational fine structure with the excitation temperature of $\sim$40 K. If we use the two-temperature populational distribution of Maier et al. (2001), i.e., $T_l = 60$ K and $T_h = 230$ K (Fig. 1*d*), or that of Roueff et al. (2002), the simulated spectrum shows a visible *R*-branch head at 4049.6 Å whose intensity is a sizable fraction of the *Q*-branch pileup (Fig. 1*d*). The absence of such an *R*-head in our observed spectrum and the narrow *Q*-branch pileup indicate that the excitation temperature of C_3 in the interstellar medium toward HD 204827 is considerably lower than toward ζ Ophiuchi and HD 210121, probably because of lower optical pumping due to higher interstellar extinction.

In the laboratory work of Gausset et al. (1965), the 000–000 origin band at 4051.6 Å is accompanied by many vibronic bands, reflecting the wide distribution of the Franck-Condon factors and the anomalously low frequency of the bending vibration $\nu_2 = 63.6$ cm^{-1} (Schuttenmaer et al. 1990). Out of those bands, hot bands starting from excited bending vibrational states are irrelevant for spectroscopy in the diffuse interstellar medium since the lifetime of the $\nu_2 = 1 \rightarrow 0$ spontaneous emission, with a theoretical transition dipole moment of 0.44 D (Jensen, Rohling, & Almlöf 1992), is on the order of 1 minute, corresponding to a critical density of $\gtrsim 10^8$ cm^{-3}. The strongest vibronic transition of relevance is therefore the 020–000 band, which Gausset et al. (1965) gave at 3991.6 Å but was later corrected to be at 3995.1 Å by Tokaryk & Chomiak (1997). Theoretical calculations have given the Franck-Condon factor of this band as 11.4% (Perić-Radić et al. 1977) and 14.3% (Jungen & Merer 1980) of that of the origin band. We simulated the spectrum of the 020–000 band using the same relative populations and Hönl-London factors as the origin band and looked for it in our observed spectrum.

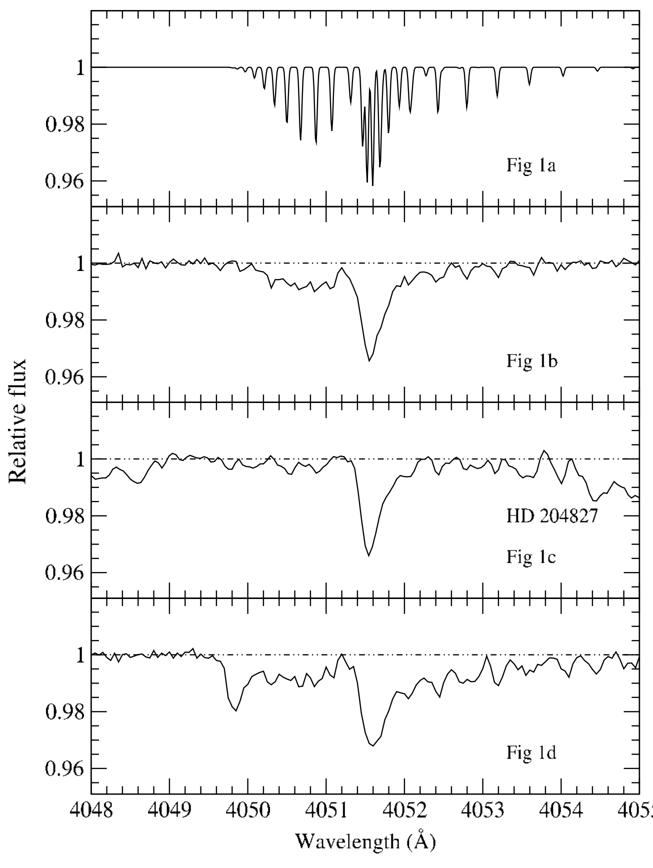

FIG. 1.—(*a*), (*b*), and (*d*) Simulated spectra of the λ4051.6 band of C_3 compared with (*c*) the observed spectrum toward HD 204827. (*a*) is for the high resolution of $R = 110,000$ and no noise, while (*b*) and (*d*) are for $R = 34,000$ and $S/N = 900$ simulating our observed conditions at the APO. A temperature of $T = 40$ K is used for (*b*), while a two-temperature distribution of $T_l = 60$ K and $T_h = 230$ K is used for (*d*) (see text).

4. RESULTS AND ANALYSIS

4.1. *Observed Spectra*

Examples of the observed C_3 spectra are shown in Figure 2. The line of sight toward HD 204827 shows by far the strongest absorption. While no C_2 observation had previously been reported, our APO spectrum has revealed a very high C_2 column density of $(4.4 \pm 0.3) \times 10^{14}$ cm^{-2} toward this star with $E(B-V) = 1.11$. This C_2 column density is comparable to that toward the much more heavily reddened star Cygnus OB2 No. 12 with $E(B-V) = 3.31$, reported to be 3.8×10^{14} cm^{-2} by Lutz & Crutcher (1983) and 3.4×10^{14} cm^{-2} by Gredel, Black, & Yan (2001). (All quoted C_2 column densities are based on an oscillator strength of 1.0×10^{-3} for the 2–0 band; van Dishoeck & Black 1989.) Evidently the interstellar gas toward HD 204827 is extraordinarily rich in carbon molecules.

In total, we have detected C_3 absorption toward 15 stars. The observed equivalent widths, W_λ, are listed in Table 2 together with the time of integration and the observed S/N in the continuum near 4051.6 Å. The uncertainties in the table correspond to 1 σ, while the upper limit corresponds to 3 σ. The W_λ values toward three stars with "$\leq$" signs represent tentative detections. Note that our W_λ values represent half of the total equivalent width of the band, since we measured only the pileup of the *Q*-branch lines (which accounts for approximately half of the total absorption). We have assembled in this table stars toward which C_3 has been detected, including those by Maier et al. (2001), and stars toward which C_2 has been detected for the first time. We have detected C_3 toward HD 179406 (20 Aql) reported by Maier et al. (2001), but we have not been able to detect C_3 toward the other two stars (ζ Oph and ζ Per) where very clear spectra of C_3 were reported by Maier et al. (2001). This indicates the lack of sensitivity of our observations (because

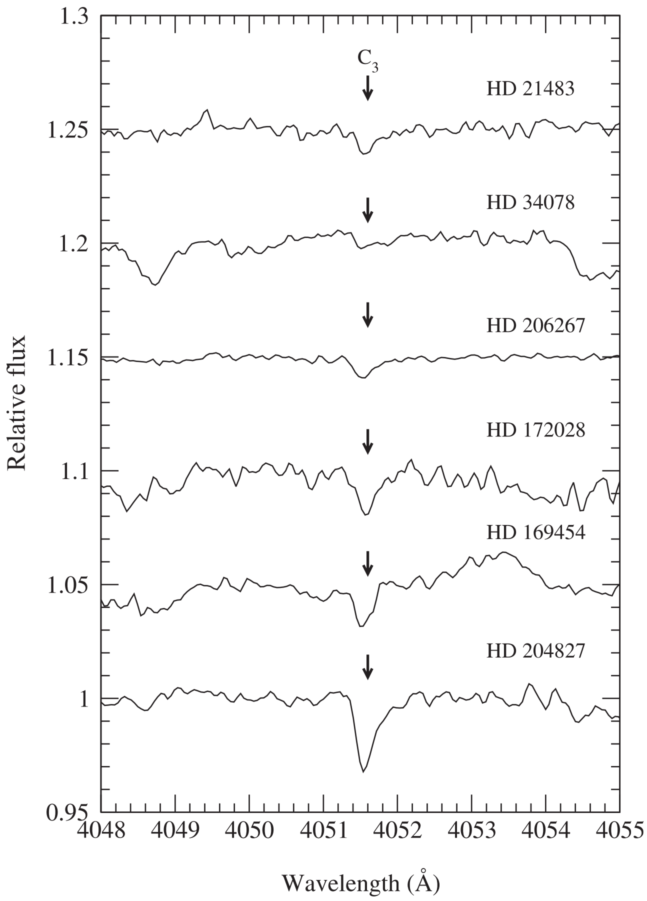

FIG. 2.—Examples of the C_3 spectrum toward six translucent sight lines.

of our lower resolution) and also illustrates the higher column densities of C_3 toward the stars where we have detected it.

There are three sight lines in which large C_2 column densities have been reported, and yet detections of C_3 are not as straightforward as in other sight lines. For HD 29647 with $N(C_2) = 1.7 \times 10^{14}$ cm^{-2} (Hobbs, Black, & van Dishoeck 1983) and HD 26571 with $N(C_2) = 1.1 \times 10^{14}$ cm^{-2} (Federman et al. 1994), narrow, blended stellar features made the detection of the weak C_3 absorption difficult and the measured column density less reliable. For HD 147889 with $N(C_2) = 1.2 \times 10^{14}$ cm^{-2} (Crutcher & Chu 1985), we set an upper limit of $W_\lambda < 3.0$ mÅ corresponding to the C_3 column density (2.6×10^{12} cm^{-2}), which is lower than the upper limit reported by Haffner & Meyer (1995; 4×10^{12} cm^{-2}).

There are 39 sight lines other than those listed in Table 2 in which the C_3 absorption was not detected. They are given in footnote a of the table with the upper limit of the equivalent width in mÅ in parentheses.

The strong C_3 and C_2 absorption toward HD 204827 prompted us to look for the 020–000 vibronic band, which is 7–9 times weaker than the 000–000 origin band as discussed in § 3. Unfortunately, the band partially overlaps with a strong stellar atomic line in HD 204827 and was not clearly detected. This band should be detectable toward stars with less atomic absorption, using higher spectroscopic resolution.

We have also looked for the spectral lines of C_4 and C_5 at 3788.6 and 5109.4 Å, respectively, which were looked for toward ζ Ophiuchi by Maier et al. (2002). The spectra have not been detected, setting the upper limit for the equivalent width of 2.6 and 1.2 mÅ (3 σ), respectively, toward HD 204728. If we use the same oscillator strengths as assumed by Maier et al. (2002), they correspond to upper limits for the C_4 and C_5 column densities of 2×10^{14} and 5×10^{12} cm^{-2} (3 σ), respectively. Maier et al. (2002) note that the λ5109 band system of C_5 is a forbidden transition and that there is a stronger band system corresponding to the $^1\Pi_u \leftarrow {}^1\Sigma_g^+$ transition that has been measured in their 5 K neon matrix at 4454 Å and is 5 times more intense than the λ5109 band. Since the gaseous wavelength of this transition is not known, we have examined spectra of HD 204827, HD 169454, HD 172028, and HD 206267, which showed strong C_3 spectra, to see if there is a matching absorption in the wavelength region from 4432 to 4476 Å (corresponding to a matrix shift of ±0.5%), without success. A gas-phase laboratory observation of this transition is eagerly waited. Although HD 204827 ($V = 7.94$) is much fainter than ζ Ophiuchi ($V = 2.56$), an order of magnitude higher observed column densities of C_2 and C_3 in HD 204827 make it a better candidate to look for C_4 and C_5 at low resolution and high sensitivity since in any case the rotational structure of the heavier carbon chains is not resolved.

4.2. *Column Density*

The C_3 column densities were obtained using the formula

$$N = \frac{2m_e c^2 W_\lambda}{\pi e^2 \lambda^2 f} = \left(2.26 \times 10^{12}\ \mathrm{cm}^{-1}\right) \frac{W_\lambda}{\lambda^2 f}$$

(Spitzer 1978). The extra factor of 2 in front of W_λ is the result of observing only the Q-branch pileup. We assume that the loss of intensity from the pileup due to Q-branch lines with high J-values that appear outside of the central feature is approximately compensated by the $P(2)$ and $P(4)$ lines that are blended in the pileup.

The value of the oscillator strength f has been controversial. Theoretical values of the oscillator strength of the electronic transition f_{1u} are converging to 0.50 (Chabalowski, Buenker, & Peyerimhoff 1986), but they are much higher than the experimental value of 0.0246 (Becker, Tatarczyk, & Perić-Radić 1979), which claims high accuracy. The Franck-Condon factor of the 000–000 band has been calculated to be 0.741 (Perić-Radić et al. 1977) or 0.615 (Jungen & Merer 1980). Here we use $f = 0.016$, which is approximately equal to the product of the experimental f_{1u} and the theoretical Franck-Condon factor, just to be consistent with Maier et al. (2001). Roueff et al. (2002) used $f = 0.0146$. Future variations of the oscillator strength will change the estimate of the column densities accordingly.

The calculated C_3 column densities are listed in Table 2. In order to explore the correlations between C_3 and other species, the observed column densities of C_2, CH, and CN are also listed in the table. For the C_2 column densities, previously reported values normalized to the oscillator strength of 1.0×10^{-3}, as well as our measured values from APO, are listed. In general they are in agreement, but some differ significantly. The CH and CN column densities have been compiled from various references in the literature or have been derived from our ARCES spectra as noted in footnote c of the table.

TABLE 2

OBSERVED DATA[a] AND DERIVED COLUMN DENSITIES OF C_3 TOGETHER WITH COLUMN DENSITIES OF C_2, CH, AND CN

Star	Name	Time (minutes)	S/N	W_λ (mÅ)	$N(C_3)$ ($\times 10^{12}$ cm^{-2})	$N(C_2)$APO[b] ($\times 10^{13}$ cm^{-2})	$N(C_2)$lit[c] ($\times 10^{13}$ cm^{-2})	N(CH)[d] ($\times 10^{13}$ cm^{-2})	N(CN)[d] ($\times 10^{13}$ cm^{-2})
HD 21483	...	88	400	2.5±0.6	2.2±0.5	11±3	9.3[e]	3.9±0.3	2.45
HD 24398	ζ Per	1.9	500	<1.8	1.0[f]	3.2±0.8	1.9±0.3[g]	2.2±0.2	0.36
HD 24534	X Per	62	350	≤1.8[h]	≤1.5[h]	7.6±2.0	5.3[i]	3.7±0.2	0.74
HD 26571	...	54	740	2.4±0.7	2.1±0.6	7.8±3.0	11[e]	2.0±0.4	0.9±0.2
HD 27778	62 Tau	80	750	1.4±0.4	1.2±0.3	6.8±1.2	3.8[e]	3.0±0.3	1.38
HD 29647	...	240	700	5.3±1.5	4.6±1.3	20±2.6	17±3[g,j]	8±2	12
HD 34078	AE Aur	45	850	2.5±0.6	2.2±0.5	10±0.9	5.8[e]	10±1	0.33
HD 149757.......	ζ Oph	3.6	800	<1.5	1.6[f]	2.5±0.7	2.4±0.3[g]	2.5±0.1	0.28
HD 169454.......	...	227	600	5.0±0.6	4.3±0.5	16±2.9	7.0±1.4[g]	3.9±0.3	4.07
HD 172028.......	...	270	300	4.2±0.7	3.6±0.6	29±2.6	19±1[k]	5.3±0.6	2.8±0.5
HD 179406.......	20 Aql	62	1000	1.5±0.8	1.3±0.7[l]	8.2±1.5	5.2[e]	2.0±0.5	0.40
HD 203938.......	...	80	550	≤1.5[h]	≤1.3[h]	7.2±1.9	...	4.1±0.4	0.35±0.04
HD 204827.......	...	570	900	12.1±0.6	10.4±0.5	44±2.9	...	8±1	5.5±0.5
HD 206267.......	...	265	1000	3.1±0.5	2.7±0.4	10±1.8	8.5±2.0[g,i]	3.0±0.3	0.81
HD 207198.......	...	95	920	1.9±0.6	1.6±0.5	9.6±0.9	3.5±0.2[g,i]	3.6±0.2	0.45
HD 210121.......	...	186	650	2.2±0.6	1.9±0.5[m]	10±1.3	6.5±1.5[n]	3.0±0.2	1.2
HD 210839.......	λ Cep	38	650	≤1.5[h]	≤1.3[h]	5.0±1.9	1.7[e,i]	2.2±0.1	0.37
HD 42087	3 Gem	25	650	<2.0	<1.7	3.8±1.0	...	1.5±0.1	0.12±0.02
HD 46202	...	180	500	<1.5	<1.3	10±1.9	...	1.7±0.3	0.16±0.04
HD 46711	...	350	350	<6	<5.2	12±2.1	...	7.4±1.1	...
HD 53367	...	60	400	<2.5	<2.2	6.1±1.6	...	4.4±0.4	0.42
HD 147888.......	ρ Oph D	91	450	<3.0	<2.6	3.9±0.7	...	2.0±0.1	0.2±0.01
HD 147889.......	...	285	225	<3.0	<2.6[o]	21±1.9	12±3[p]	10±1	3.47
HD 170740.......	...	40	650	<1.5	<1.3	2.4±1.4	...	2.1±0.2	0.87

[a] Nondetections of C_3 in sight lines not listed in this table (with the upper limit of equivalent width in mÅ in parentheses) are as follows: HD 11415 (1.5), HD 20041 (2.5), HD 21389 (3.0), HD 23180 (1.8), HD 281159 (2.5), HD 24912 (1.5), HD 30614 (1.5), HD 35149 (1.5), HD 36371 (1.5), HD 37022 (5.0), HD 37903 (1.5), HD 41117 (2.0), HD 42690 (3.0), HD 43384 (3.0), HD 46056 (6.0), HD 47839 (2.0), HD 48099 (1.5), HD 50064 (4.0), HD 74280 (3.0), HD 87887 (4.0), HD 91316 (2.0), HD 93521 (3.0), HD 143275 (1.0), HD 147933 (1.5), HD 164353 (3.0), HD 166734 (3.0), HD 167971 (3.0), HD 168076 (3.0), HD 176437 (3.0), HD 183143 (3.0), HD 185418 (1.5), HD 186994 (2.0), HD 192639 (2.0), HD 229059 (3.0), HD 198478 (1.0), HD 199579 (1.5), HD 206165 (1.5), HD 218376 (1.4), BD +63° 1964 (4.0).

[b] C_2 column densities observed at APO.

[c] C_2 column densities reported previously. The values are normalized to the oscillator strength of $f = 1.0 \times 10^{-3}$.

[d] References for some of the CH and CN column densities are given in Welty & Hobbs 2001 and D. E. Welty, T. P. Snow, and D. C. Morton (2003, in preparation); other values have been derived from our ARCES spectra.

[e] Federman et al. 1994.

[f] Maier et al. 2001.

[g] van Dishoeck & Black 1989.

[h] Tentative detections.

[i] Federman & Lambert 1988.

[j] Hobbs et al. 1983.

[k] Gredel 1999.

[l] Maier et al. 2001 give 2.

[m] Roueff et al. 2002 give 3.8.

[n] Gredel et al. 1992.

[o] Haffner & Meyer 1995 give less than 4.

[p] van Dishoeck & de Zeeuw 1984.

4.3. *Correlations*

Correlation diagrams between the observed column densities of C_3 and those of C_2, CH, and CN as well as the color excess $E(B-V)$ are shown in Figure 3. The top left-hand panel of Figure 3 shows the correlation between $N(C_3)$ and $N(C_2)$. Column densities of C_2 derived from our APO spectra are used for consistency. It is clear from this figure that $N(C_3)$ and $N(C_2)$ are well correlated. In the eight sight lines that show C_3 column densities higher than 2×10^{12} cm^{-2}, the observed ratio of $N(C_2)$ to $N(C_3)$ falls within 42 ± 8 with the sole exception of HD 172028, for which the ratio is 81. The correlation coefficient is 0.932. This supports the expected close relation between the chemistry of C_2 and C_3 in the diffuse interstellar medium. The correlations between $N(C_3)$ and N(CH) and N(CN) given in the top right-hand and bottom left-hand panels of Figure 3, respectively, are not as good, with correlation coefficients of 0.576 and 0.626, respectively.

The C_3 column densities and the color excess shown in the bottom right-hand panel of Figure 3 have a correlation coefficient of 0.728. In this figure we use only sight lines where C_3 has been detected; if we take into account other sight lines, the correlation coefficient is considerably lower. There are carbon-poor sight lines with high $E(B-V)$ and strong diffuse interstellar absorption bands (DIBs) but with no detectable C_2 and C_3, such as toward HD 183143 [$E(B-V) = 1.27$] and HD 20041 [$E(B-V) = 0.72$]. It is interesting to note that high column densities of H_3^+, 2.3×10^{14} cm^{-1} and 3.5×10^{14} cm^{-2}, respectively, have been observed along those two lines of sight (McCall et al. 2002). This indicates that the chemistry of C_2 and C_3 is completely decoupled from the chemistry of H_3^+. Our extensive data set of the DIBs has

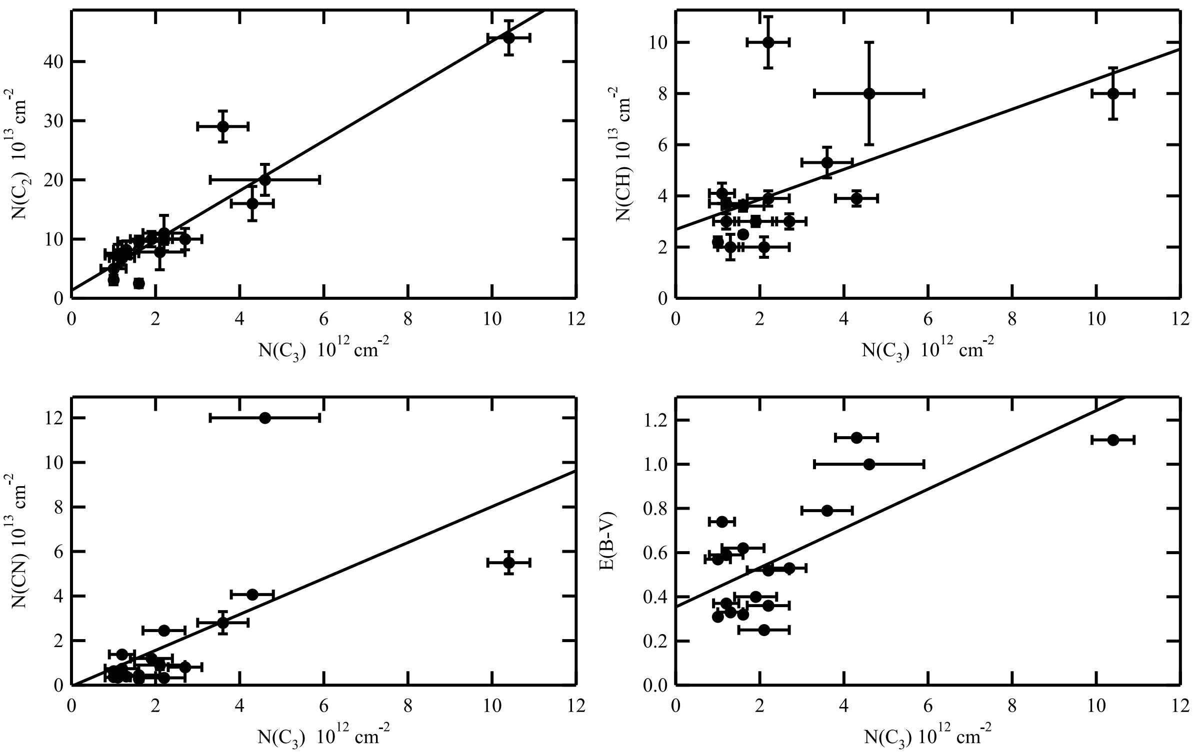

FIG. 3.—Correlation diagrams between the observed column densities of C_3 and those of C_2 (*top left*), CH (*top right*), CN (*bottom left*), and the color excess $E(B-V)$ (*bottom right*). The correlation coefficients are 0.932, 0.576, 0.626, and 0.728, respectively.

led to the observation that there is a family of DIBs that is enhanced in the lines of sight with high C_2 and C_3 column densities. These findings are discussed in a separate paper (Thorburn et al. 2003).

5. CHEMISTRY OF C_3

The observed strong correlation between $N(C_3)$ and $N(C_2)$ suggests that C_3 and C_2 are in the same chain of chemical reactions. Based on previous studies of the chemistry of C_3 (Mitchell, Ginsburg, & Kuntz 1978; Clegg & Lambert 1982), the following chains of reactions are considered (see Fig. 4).

These chains of reactions include four types of chemical reactions involving the three abundant chemically active species in the diffuse interstellar medium (H_2, C^+, and electrons) as well as photons. To obtain an order-of-magnitude estimate of the various reaction rates, we assume typical number densities of $n(H_2) = 10^2$ cm^{-3} and $n(C^+) = n(e) = 10^{-2}$ cm^{-3}. We also adopt the general Langevin rate constant of 10^{-9} cm^3 s^{-1} for ion-neutral reactions and an electron recombination rate constant of 10^{-7} cm^3 s^{-1}. The

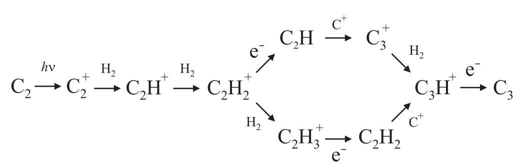

FIG. 4.—Formation of C_3 from C_2 by photoionization, ion neutral reactions, and dissociative recombinations.

hydrogen abstraction reaction

$$X^+ + H_2 \rightarrow XH^+ + H$$

is the fastest with a rate of $\sim 10^{-7}$ s^{-1} except for $X^+ = C_2H_2^+$, $C_2H_3^+$, and C_3H^+, which will be discussed below. The electron recombination reaction

$$XH^+ + e \rightarrow X + H$$

is next with a rate of $\sim 10^{-9}$ s^{-1}, and the chain building reaction

$$XH + C^+ \rightarrow XC^+ + H$$

is the slowest, with a rate of $\sim 10^{-11}$ s^{-1}. The photoionization rate of C_2 seems to be poorly determined, but an estimate of $10^{-10} \exp(-2A_v)$ s^{-1} has been used (Mitchell et al. 1978).

Hydrogen abstraction reactions of three carbocations have especially low rates, and their competition with the electron recombination rate has to be considered separately. The reaction of $C_2H_3^+$ is highly endothermic ($\sim$2.7 eV), and its rate is negligible. The rate constant of the reaction

$$C_2H_2^+ + H_2 \rightarrow C_2H_3^+ + H$$

has been controversial. If we use the rate reported by Smith & Adams (1977), which is lower than the Langevin rate by 2 orders of magnitude, the reaction is competitive with the dissociative recombination of $C_2H_2^+$ and hence the branching of the chain in Figure 4. Ab initio theory even predicts that the reaction is slightly (0.08 ± 0.08 eV) endothermic (Maluendes, McLean, & Herbst 1994) although there is a conflicting experimental report (Hawley & Smith 1992).

Future astronomical observations of either C_2H or C_2H_2 in the chain may settle this controversy. The reaction

$$C_3H^+ + H_2 \rightarrow C_3H_2^+ + H$$

has been shown to be slightly endothermic and slower than the radiative association reaction

$$C_3H^+ + H_2 \rightarrow C_3H_3^+ + h\nu$$

by Maluendes, McLean, & Herbst (1993). The rate of this reaction, 9×10^{-12} cm^3 s^{-1} (E. Herbst 2002, private communication), is slower than the electronic recombination, but this reaction may be an important channel to cyclic C_3H_2 (Maluendes et al. 1993).

In the chemical flow chart of Figure 4, molecules with a low destruction rate (i.e., by chain building with C^+ and photoionization) are abundant. Simple steady state chemical kinetics indicate that the neutral molecules C_2, C_2H, C_2H_2, and C_3 (the main destruction mechanism of C_3 is photoionization/dissociation) are more abundant than the ionic species by at least 2 orders of magnitude. It will be interesting to observe C_2H in the radio and/or C_2H_2 in the ultraviolet in the same sight lines where C_2 and C_3 have been observed.

The flow of chain reactions is reduced at each juncture by other reactions that branch out from it. They include photodissociation and ionization, electron recombination, reactions with oxygen atoms, and other ion-neutral reactions. The small value of $N(C_3)/N(C_2) \sim 1/40$ is due to those reductions and the photodissociation of C_3 back to C_2.

6. SUMMARY

We have detected the C_3 λ4051.6 spectrum in 15 translucent sight lines. The observed C_3 column densities range from 1.0×10^{13} to 1.2×10^{12} cm^{-2}. As expected, the observed C_3 column densities are well correlated with the C_2 column densities with $N(C_2)/N(C_3)$ falling in 42 ± 8 for all strong signals except one. The observation has revealed HD 204827 to be by far the most carbon-rich sight line, which makes it a good candidate to search for higher carbon chain molecules. For HD 206267, HD 207198, and HD 210121, for which column densities of both H_2 and H have been measured, the fractional abundances of C_3 are $x(C_3) \times 10^{10}$ = 7.9, 4.4, and 11, respectively. It is interesting to study observationally and theoretically how carbon chains grow from C_3. Elongation of carbon chains using direct C^+ association followed by hydrogen abstraction reactions and recombination is slow for simple carbon molecules, but it becomes increasingly fast after C_4 (Freed, Oka, & Suzuki 1982).

This work is based on observations obtained with the Apache Point Observatory 3.5 m telescope, which is owned and operated by the Astrophysical Research Consortium. T. O. wishes to thank E. Herbst for several clarifying discussions on the ion chemistry of hydrocarbons. T. O. acknowledges support from NSF grants PHY-9722691 and PHY-0099442, and D. E. W. acknowledges support from NASA LTSA grant NAG5-3228. B. J. M. has been supported by the Miller Institute for Basic Research in Science.

REFERENCES

Becker, K. H., Tatarczyk, T., & Perić-Radić, J. 1979, Chem. Phys. Lett., 60, 502
Bobrovnikoff, N. T. 1931, ApJ, 73, 61
———. 1942, Rev. Mod. Phys., 14, 164
Cernicharo, J., Goicoechea, J. R., & Caux, E. 2000, ApJ, 534, L199
Chabalowski, C. F., Buenker, R. J., & Peyerimhoff, S. D. 1986, J. Chem. Phys., 84, 268
Chaffee, F. H., Jr., & Lutz, B. L. 1978, ApJ, 221, L91
Clegg, R. E. S., & Lambert, D. L. 1982, MNRAS, 201, 723
Crampton, D., Cowley, A. P., & Humphreys, R. M. 1975, ApJ, 198, L135
Crawford, I. A. 1990, MNRAS, 244, 646
Crutcher, R. M., & Chu, Y.-H. 1985, ApJ, 290, 251
Douglas, A. E. 1951, ApJ, 114, 466
Federman, S. R., & Lambert, D. L. 1988, ApJ, 328, 777
Federman, S. R., Strom, C. J., Lambert, D. L., Cardelli, J. A., Smith, V. V., & Joseph, C. L. 1994, ApJ, 424, 772
Freed, K. F., Oka, T., & Suzuki, H. 1982, ApJ, 263, 718
Gausset, L., Herzberg, G., Lagerqvist, A., & Rosen, B. 1963, Discuss. Faraday Soc., 35, 113
———. 1965, ApJ, 142, 45
Geballe, T. R., McCall, B. J., Hinkle, K. H., & Oka, T. 1999, ApJ, 510, 251
Giesen, T. F., van Orden, A. O., Cruzan, J. D., Provencal, R. A., Saykally, R. J., Gendriesch, R., Lewen, F., & Winnewisser, G. 2001, ApJ, 551, L181
Gredel, R. 1999, A&A, 351, 657
Gredel, R., Black, J. H., & Yan, M. 2001, A&A, 375, 553
Gredel, R., van Dishoeck, E. F., de Vries, C. P., & Black, J. H. 1992, A&A, 257, 245
Haffner, L. M., & Meyer, D. M. 1995, ApJ, 453, 450
Hawley, M., & Smith, M. A. 1992, J. Chem. Phys., 96, 1121
Hinkle, K. H., Keady, J. J., & Bernath, P. F. 1988, Science, 241, 1319
Hobbs, L. M. 1979, ApJ, 232, L175
Hobbs, L. M., Black, J. H., & van Dishoeck, E. F. 1983, ApJ, 271, L95
Hrivnak, B. J., & Kwok, S. 1999, ApJ, 513, 869
Huggins, W. 1881, Proc. R. Soc. London A, 33, 1
Huggins, W. 1882, Proc. R. Soc. London A, 34, 148
Jensen, P., Rohling, C. M., & Almlöf, J. 1992, J. Chem. Phys., 97, 3399
Jørgensen, U. G. 1994, in Molecules in the Stellar Environment, ed. U. G. Jørgensen (Berlin: Springer), 29
Jungen, Ch., & Merer, A. J. 1980, Mol. Phys., 40, 95
Lutz, B. L., & Crutcher, R. M. 1983, ApJ, 271, L101
Maier, J. P., Lakin, N. M., Walker, G. A. H., & Bohlender, D. A. 2001, ApJ, 553, 267
Maier, J. P., Walker, G. A. H., & Bohlender, D. A. 2002, ApJ, 566, 332
Maluendes, S. A., McLean, A. D., & Herbst, E. 1993, ApJ, 417, 181
———. 1994, Chem. Phys. Lett., 217, 571
McCall, B. J., Geballe, T. R., Hinkle, K. H., & Oka, T. 1998, Science, 279, 1910
McCall, B. J., et al. 2002, ApJ, 567, 391
McKellar, A. 1948, ApJ, 108, 453
Mitchell, G. F., Ginsburg, J. L., & Kuntz, P. J. 1978, ApJS, 38, 39
Perić-Radić, J., Römelt, J., Peyerimhoff, S. D., & Buenker, R. J. 1977, Chem. Phys. Lett., 50, 344
Roueff, E., Felenbok, P., Black, J. H., & Gry, C. 2002, A&A, 384, 629
Schuttenmaer, C. A., Cohen, R. C., Pugliano, N., Heath, J. R., Cooksy, A. L. Busarow, K. L., & Saykally, R. J. 1990, Science, 249, 897
Smith, D., & Adams, N. G. 1977, Chem. Phys. Lett., 47, 383
Snow, T. P., Seab, C. G., & Joseph, C. L. 1988, ApJ, 335, 185
Souza, S. P., & Lutz, B. L. 1977, ApJ, 216, L49
Spitzer, L., Jr. 1978, Physical Processes in the Interstellar Medium (New York: Wiley)
Thorburn, J. 2000, UC Data Reduction Guide II
Thorburn, J. A., et al. 2003, ApJ, in press
Tokaryk, D. W., & Chomiak, D. E. 1997, J. Chem. Phys., 106, 7600
van Dishoeck, E. F., & Black, J. H. 1982, ApJ, 258, 533
———. 1986, ApJS, 62, 109
———. 1989, ApJ, 340, 273
van Dishoeck, E. F., & de Zeeuw, P. T. 1984, MNRAS, 206, 383
Wang, S., et al. 2002, Proc. SPIE, in press
Welty, D. E., & Hobbs, L. M. 2001, ApJS, 133, 345